Multiscale Voltage Reconstruction with Attention-based network for Volume Fraction Prediction of Industrial Oil-Water Two-Phase Flow by EIT

Citation for published version:
Yu, H, Zhang, Z, Gao, Y & Jia, J 2022, 'Multiscale Voltage Reconstruction with Attention-based network for Volume Fraction Prediction of Industrial Oil-Water Two-Phase Flow by EIT', *IEEE Transactions on Instrumentation and Measurement*, vol. 71, 4503409, pp. 1-9. https://doi.org/10.1109/TIM.2022.3169557

Digital Object Identifier (DOI):
10.1109/TIM.2022.3169557

Published In:
IEEE Transactions on Instrumentation and Measurement

Multiscale Voltage Reconstruction with Attention-based network for Volume Fraction Prediction of Industrial Oil-Water Two-Phase Flow by EIT

Hao Yu, Zhixi Zhang, Yang Gao, Jiabin Jia, *Senior Member*, *IEEE*

***Abstract*— Oil-water two-phase flow as a typical two-phase flow type widely exists in various industrial processes and the accurate measurement of oil volume fraction plays a significant role in transporting and separating oil-water mixture in the processes. Electrical Impedance Tomography (EIT) as a merging technology with the advantages of non-invasive, low cost and real-time measurement is widely applied in the industrial field to measure the volume fraction for different types of two-phase flows. However, the measurement process of taking homogeneous reference voltages is time-consuming and costly. To cope with the problem, in the paper, by establishing an end-to-end mapping between measurement voltages and volume fraction, we propose an Attention UNet-Fully Connected (AU-FC) architecture. Relying on the attention mechanism, the reconstructed voltages having a strong correlation or a weak correlation with volume fraction is highlighted or suppressed respectively. Oil-water two-phase flow experiment was conducted in the NEL facility to collect EIT voltage data. Compared with six state-of-the-art and existing machine learning methods, the proposed method performs better in predicting volume fraction. The results indicate that the proposed AU-FC architecture can accurately and real-time predict the volume fraction of oil-water two-phase flow, which improves the application potential of EIT combined with deep learning method in the industrial field.**

***Index Terms*—Electrical impedance tomography (EIT), oil-water two-phase flow, attention mechanism, volume fraction, deep learning.**

I. Introduction

OIL-WATER two-phase flow wildly exists and of great importance in the industrial field, such as drug production and petroleum exploit [1], [2]. Different from single-phase flow, two-phase flow has flow characteristics such as inter-phase relative velocity, inter-phase slip and nonlinear response [3]. Due to the complexity, randomness and uncertainty of oil-water two-phase flow behavior, it brings difficulty in measuring the flow parameters, such as Volume Fraction (VF) [4], which, as a typical parameter, plays a critical role in industrial process control and optimization of the production process [5]–[7]. Therefore, accurate measuring the oil volume fraction of oil-water two-phase flow has attracted increasing attention in industrial and academic fields.

Yu *et al.* [8] established a fractal-based modified attenuation model to estimate the oil VF of oil-water two-phase flow using the ultrasonic sensor. The effectiveness of the model was validated by numerical simulation and experiment results. Zhang *et al.* [9] utilized the differential pressure sensors and the mathematical relationship between volume fraction and difference between oil and water densities to calculate the dispersed volume fraction of oil-water two-phase flow. By combing the long-waist cone meter with the conductance ring coupled cone meter, Tan *et al.* [10] accurately measured the volume fraction. Sharifzadeh [11] *et al.* used a pencil-beam collimated gamma-ray to measure the VF.

Electrical impedance tomography, as a merging and promising visual imaging technology, has been widely used in two-phase flows for estimating volume fraction due to the advantages of real-time non-invasive monitor, easy installation, safety, and low cost [12]–[14]. By adjacent excitation and adjacent measurement patterns, EIT can obtain the boundary voltages of the pipeline, and non-iterative algorithms such as Tikhonov [15], Linear Back Projection (LBP) [16] and Newton's One-step Error Reconstructor (NOSER) [17] could be used to real-time reconstruct the conductivity distribution, and then the dispersed phase volume fraction can be obtained according to the Maxwell equation [18]. In gas-water two-phase flow, with VF less than 30%, the VF measured by EIT is consistent with that of the wire-mesh sensor (WMS), a sensor with the excellent agreement to the VF measured by Electrical Capacitance Tomography (ECT) for an air/silicone oil flow [19]. Xu *et al.* designed a EIT device with 12 contactless sensors to collect raw data of gas–liquid two-phase flow and the volume fraction of three different flow types was estimated by data average method using five-electrode excitation pattern. Compared with the reference, the absolute error values are less than 5% [20]. Besides, for highly conductive oil-water two-phase flow, the VF measured by EIT also has a great agreement with VF provided by NEL with error in ± 3% [12].

However, when applying EIT in the industrial field, prior information needs to be known that the pipeline needs to be fully filled with the single-continuous phase medium in advance to measure the reference voltages, a critical variable

(Corresponding author: Jiabin Jia).
Hao Yu, Zhixi Zhang, Yang Gao and Jiabin Jia are with Agile Tomography Group, School of Engineering, Institute for Digital Communications, The University of Edinburgh, Edinburgh, EH9 3JL, U.K., (e-mail: jiabin.jia@ed.ac.uk).

for conductivity reconstruction, which is time-consuming and costly, even impossible to be executed. Besides, with the change in temperature and other factors, reference voltages will also vary with time, which hinders the accuracy of collecting voltages. Estimating reference voltages seems to be an effective way to cope with the problem. Wang *et al.* [21] used the Measurement-Scale Feature (MSF) method to estimate the reference voltages, however, the estimation accuracy in oil-water two-phase flow cannot be guaranteed and even if the reference voltage is accurately estimated, the accumulation of its errors will result in the obtained volume fraction to be inaccurate.

In recent years, with the explosive growth of data volume and the significant improvement in hardware performance, the deep learning, as a kind of representative machine learning method, generates an overwhelming enthusiasm in solving all kinds of nonlinear problems related to two-phase flows. For example, Gao *et al.* [22] proposed a Convolutional Neural Network (CNN) based temporal-channel-wise architecture to extract information from measurement currents to predict the gas void fraction and its category. Tan *et al.* [23] established a sparse batch normalization CNN framework to reconstruct the interface image of gas-liquid two-phase flow. Azizi *et al.* [24] employed Probabilistic Neural Network (PNN) and Multilayer Perceptron (MLP) network to predict the oil VF and flow patterns. Dang *et al.* [25] combined CNN with long short-term memory (LSTM) to extract time-dependent sensor information to predict flow parameters. Aiming at solving the ECT ill-posed problem of the image reconstruction for solid-gas two-phase flow, Chen *et al.* used an improved radial basis function (IRBF) network to get the initial reconstruction results, followed by the adaptive wavelet image enhancement technique to enhance the quality of images [26]. The pre-reconstruction and post-processing process makes the method complex. Combing with the reference provided by air-filled sensor, Zhang *et al.* proposed a CVMF-ECT method based on deep network to reconstruct the air-water two-phase flow distribution [27]. Two-layer ECT was applied to collect the boundary voltages to predict the oil, gas flow rate and gas VF by CNN network [28]. Although the design of multi-layer convolutional connections network is simple, the problems of computational depth and performance degradation of the models are not addressed. All these contributions have confirmed the reliability and validity of deep learning method in solving two-phase flow regression and classification problems.

In this paper, inspired by [29], which introduced attention module in skip connection part of UNet network and [30], which proposed attention mechanism for EIT cell image reconstruction, a soft measure data-driven deep learning model: Attention UNet Fully Connected (AU-FC) model is proposed to directly predict the volume fraction of oil-water two-phase flow from the measurement voltages. The network uses the attention mechanism to strengthen the reconstructed multiscale voltages and accurately predicts the oil volume fraction through the fully connected layers. The experiments were carried out to establish the data set, and compared with the six competitive methods, the proposed model outperforms other methods. The main contributions of the work are as follows: 1) a novel network with the attention mechanism is proposed to perform voltage reconstruction to predict oil volume fraction of oil-water two-phase flow. 2) The proposed regression network has good accuracy and has excellent prediction performance in the constructed data set. The work shows the feasibility of real-time online monitoring for the oil volume fraction using the deep learning method and provides the preliminary theoretical basis and experimental verification for the application of EIT combined with deep learning in two-phase flow. Besides, the designed attention network may also be suitable for the conductivity and permittivity reconstruction of EIT and ECT. Also, it can be used to predict the volume fraction of the multiphase flow with a slight change of the network.

The structure of the paper is organized as follows. Section II details the measurement principle of volume fraction by EIT and proposes the AU-FC architecture to predict volume fraction. Also, the section presents six competitive methods as baselines. Section III introduces the experiment setup process and details the data normalization and training setting. Section IV compares the prediction performance under different methods. Finally, Section V gives a brief summary.

II. METHODS

In this section, the volume fraction measurement method by EIT is introduced and a deep learning method: AU-FC is proposed to reconstruct multiscale voltages to predict volume fraction. The loss function is described. Besides, to reveal the superiority of the proposed architecture, six state-of-the-art and competitive methods are described.

A. EIT Volume Fraction

By EIT, the relative conductivity distribution of dispersed phase, such as oil, and continuous phase, e.g., water can be obtained in two-phase flow as shown in Fig. 1. The blue patch represents the continuous phase (water) and the gray represents the dispersed phase (oil). Due to the conductivity difference of two-phase flow, the Maxwell relationship [18] can be used to calculate pixel volume fraction as follows,

$$\alpha_i = \frac{2-2\frac{\sigma_i}{\sigma_1}}{2+\frac{\sigma_i}{\sigma_1}} \tag{1}$$

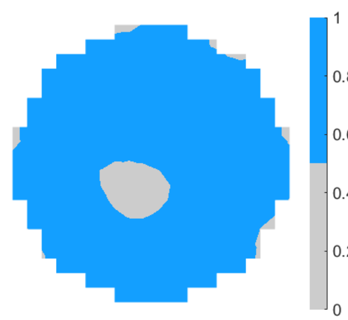

Fig.1. The reconstructed relative conductivity distribution of the oil-water two-phase flow.

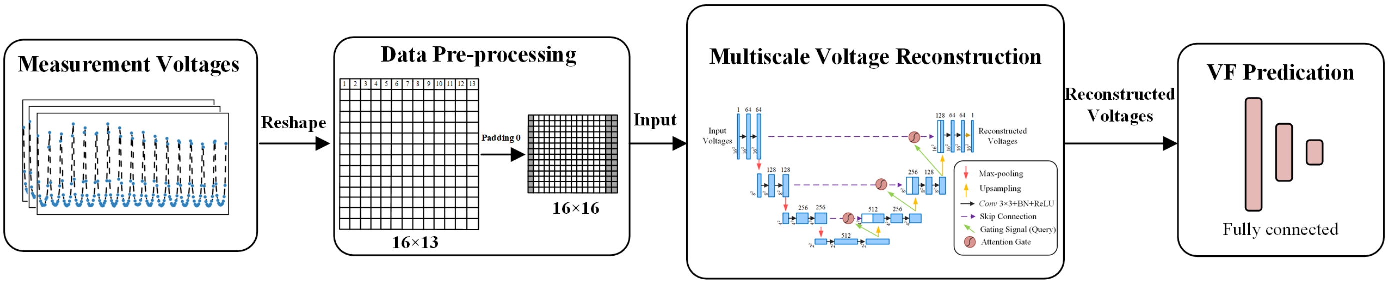

Fig.2. Architecture of the AU-FC Network.

where α_i is i-th pixel VF and the frame VF is the average VF of total pixels in one frame, which is 316 in the paper. σ_i is the mixture conductivity obtained from EIT and σ_1 is the conductivity of continuous phase (water). The ratio of σ_i/σ_1, a 316×1 vector, is the only variable in the equation (1).

Modified Sensitivity Back Projection (MSBP) [31] algorithm, as a common non-iterative EIT reconstruction method, is adopted to reconstruct the relative conductivity change and the expression is as follows,

$$\frac{\sigma_i}{\sigma_1} \approx \frac{1}{S^T \cdot (U_{Mea} / U_{Ref})} \tag{2}$$

where S is the sensitivity matrix, also called the Jacobin matrix, U_{Mea} and U_{Ref} are the measurement and reference voltages, respectively.

To mitigate the variation error of frame VF, in the paper the average of 2000 frames is used as the measurement VF.

B. Attention-UNet Fully Connected Network

In the paper, our goal is to establish an end-to-end nonlinear mapping between measurement voltages and volume fraction of oil-water two-phase flow, and the task can be converted into the following mathematical problem,

$$f = \arg\min_{\theta} \frac{1}{N} \sum_{k=1}^{N} \left\| f\left(U_{Mea}\right) - \alpha \right\|_2^2 + \lambda \left\|\theta\right\|_2^2 \tag{3}$$

where f is the AU-FC network model, $f(U_{Mea})$ is the predicted volume fraction, α is the volume fraction measured by EIT and the latter term is the l_2 regularization with regularization parameter λ. $\theta = \{W, b\}$ denotes the training parameters: weights and bias of the network, N represents the total sample number in the training set.

TABLE I

OUTPUT SIZE OF THE PROPOSED AU-FC

Layers	AU-FC	Output size
Input	\	1×208
Data Pre-processing Block	Reshape Padding 0	16×13 16×16
Multiscale Voltage Information Reconstruction Block	Conv 3×3+ Skip connection+ Attention gate Maxpooling Up-sampling	16×16×1
Volume Fraction Block (Output)	Flatten Fully connected Fully connected	1×256 1×104 1×1

*Height×Width×Channel

The architecture of AU-FC is shown in Fig. 2 and the detailed dimension change of voltages for the proposed architecture is shown in Table I. Before inputting the measurement voltages which are without reference voltages into the network, the voltages should be preprocessed to adapt to the network structure. Inspired by [32], the 1×208 voltage vector is reshaped to a 16×13 voltage matrix, and each row represents the induced voltage between adjacent electrodes under the excitation of the specified electrode. Then, the 16×13 voltage matrix is projected into a 16×16 voltage matrix by padding 0 to the three columns in gray. After the multiscale voltage, a 16×16 matrix is reconstructed by the attention UNet, a fully connection layer is followed with 256, 104 and 1 dimensions to predict the volume fraction for oil-water two-phase flow.

The detailed structure of the multiscale voltage

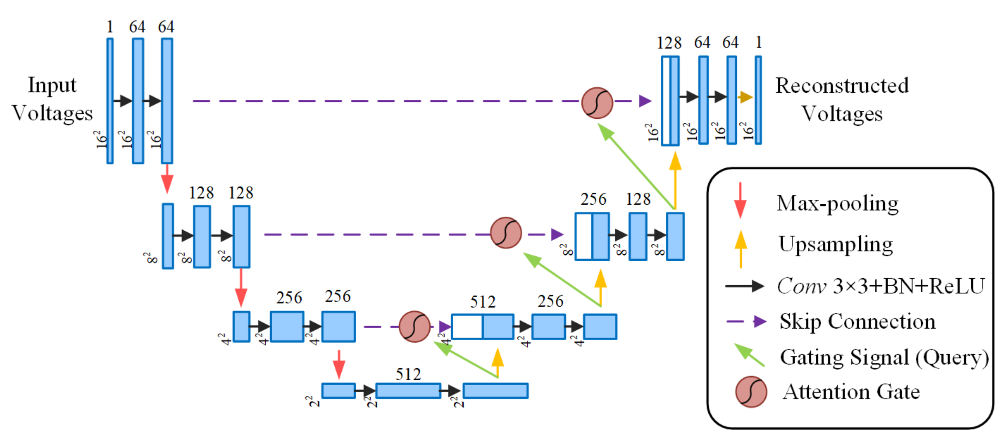

Fig.3. Architecture of the multiscale voltage reconstruction block.

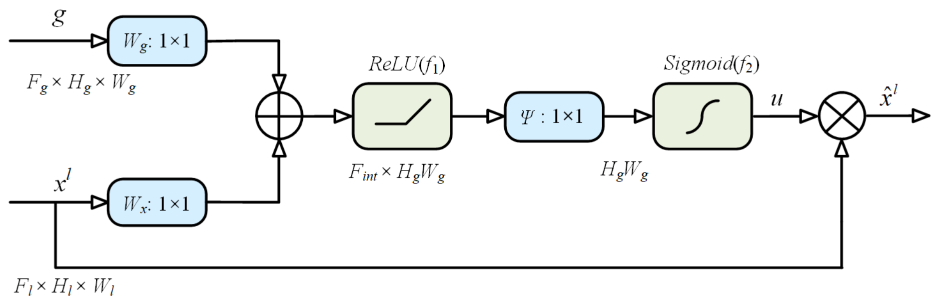

Fig.4. Structure of the attention gate.

reconstruction block is shown in Fig. 3. The network is built based on the UNet structure. After data pre-processing block, the 16×16 voltage matrix is operated by two 3×3 convolution layers and a 2×2 maxpooling layer in each step. After three identical operation steps, the bottom layer passes through a 2×2 up-sampling layer, and similarly, followed by two 3×3 convolution layers with also three same steps. Finally, at the last step, a 1×1 kernel is adopted to adjust the number of output channels, followed by a Sigmoid activation function to reconstruct the voltages,

$$S(x) = \frac{1}{1+e^{-x}} \tag{4}$$

where x is the input of the Sigmoid function, and $S(x)$ is the output of the function.

Besides, the attention mechanism module is added to the skip connection part of the traditional UNet network, and the additive spatial self-attention mechanism module can enhance the feature learning ability of the network for EIT measurement voltages, so that the reconstructed voltage can extract more scale information, thereby improving the accuracy of the volume fraction prediction rate and reducing prediction error.

The additive attention gate in the skip-connection part is shown in Fig. 4. F represents the feature map number, and H, W are the height and width of the voltage matrix. The attention gate could filter the neuron activations during both forward and backward passes, and mathematical expressions of the gate are as follows,

$$q_{att}^l = \psi^T \left(f_1 \left(W_x^T x_i^l + W_g^T g_i + b_x + b_g \right) \right) + b_\psi \tag{5}$$

where W_x and W_g are the feature weight matrix, x_i^l and g_i are the encoder and decoder matrix. f_1 is the ReLU activation function, ψ is the convolutional operator with 1×1 kernel. b_x, b_g and b_ψ are the bias terms of the corresponding convolutional operation. q_{att}^l is the intermediate matrix.

The attention coefficient $u_i^l \in [0,1]$ is defined as follows,

$$u_i^l = f_2 \left(q_{att}^l \left(x_i^l, g_i; \Theta_{att} (W_x, W_g, \psi, b_x, b_g, b_\psi) \right) \right) \tag{6}$$

where f_2 is the Sigmoid function, Θ_{att} represents a set of parameters containing W_x, W_g, ψ, b_x, b_g and b_ψ.

The attention gate output $\hat{x}_i^l$ is the element-wise multiplication of attention coefficient u_i^l and encoder matrix x_i^l. By multiplication as shown in equation (7), the weight of the EIT voltages that has a strong correlation with the volume fraction would be increased, and oppositely, the weight of voltages with weak impact would be decreased. The output obtained is the multiscale reconstruction voltage with the attention mechanism.

$$\hat{x}_i^l = u_i^l \odot x_i^l \tag{7}$$

The AU-FC network makes use of the weighting method to extract the characteristic voltages of different depths obtained in the encoding part, and then concats with the characteristic voltages of halved dimensions obtained by upsample layers to reconstruct the specific details of the voltages, so as to achieve the selective and full extraction of the voltage features.

C. Loss Function

In the paper, the hybrid loss function is adopted and described by,

$$L_{\text{Total}} = \beta L_{\text{MAPE}} + \gamma L_{\text{MAE}} \tag{8}$$

where β and γ are the loss function component weights. L_{Total} is the total loss. L_{MAE} is the Mean Absolute Error (MAE) loss component. L_{MAPE} is the Mean Absolute Percentage Error (MAPE) loss component. They are described as follows,

$$MAE = \frac{1}{N} \sum_i^N \left| \hat{\alpha}_i - \alpha_i \right| \tag{9}$$

$$MAPE = \frac{100\%}{N} \sum_{i=1}^N \left| \frac{\hat{\alpha}_i - \alpha_i}{\alpha_i} \right| \tag{10}$$

where $\hat{\alpha}_i$ is the predicted volume fraction and α_i is the reference volume fraction calculated by EIT.

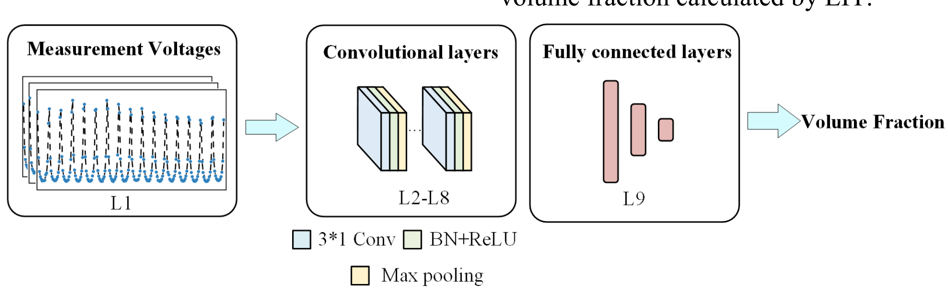

Fig.5. Architecture of the MLCNN Network.

Larger weights represent that the corresponding loss term is more critical to the total loss function, and after a series of careful experiments with a purpose to balance MAE and MAPE metrics, β and γ are set to 0.2 and 1, respectively.

D. *Model Comparisons*

To reveal the superiority of the AU-FC architecture, different state of art and existing machine learning methods are presented, and the brief introduction of the methods are as follows.

Support Vector Regression (SVR): SVR [33] is one category of Support Vector Machine (SVM) to deal with regression tasks, and the mathematical model $f_{SVR}(x)$ is described as follows,

$$f_{SVR}(x)=\sum_{i=1}^{N}\left(o_i-o_i^*\right)K\left(x_i,x\right)+b \tag{11}$$

where $K(x_i, x)$ is the kernel function, o_i and o_i* are the Lagrange multiplier, and b is the bias. In the paper, we select Gaussian kernel, also called Radial Basis Function (RBF) kernel as kernel function.

LeNet: LeNet [34] is a typical CNN-based model with two convolution-maxpooling layers, followed by fully connected layers and a Sigmoid activation function. Referring to [32], to adapt the EIT regression problem, the Sigmoid function is replaced with the ReLU function.

Multilayers Convolutional Neural Network (MLCNN): MLCNN as shown in Fig. 5 is improved based on VGG architecture [35], with 7 similar sequential blocks, consisting of a 3×3 convolution kernel, a Batch Normalization (BN) layer, a maxpooling layer and a ReLU activation function, to extract EIT voltages information, finally followed by FC layers and a ReLU activation function.

ResNet: ResNet18 [36] proposes 18 layers to extract deep network information. By residual learning, the degradation problem of the network can be solved. In the paper, ResNet18 is selected as backbone, followed by FC layers to predict volume fraction.

Fully Connected (FC): To validate the effectiveness of reconstructed multiscale voltages process, after preprocessing the input voltages into 16×16 matrix, FC layers are directly connected with the voltage matrix.

UNet- Fully Connected (UNet-FC): we choose the UNet architecture mentioned in [37] as the backbone, after reconstructing multiscale voltages, the FC mentioned above is connected with UNet to predict volume fraction.

III. EXPERIMENT SETUP

In this section, information about the TUV NEL facility is introduced, and three regression metrics are used in the paper to evaluate the prediction performance under different methods. Finally, the hyperparameter setting is described.

A. *Experiment Setup*

The schematic of NEL two-phase flow facility is shown in Fig. 6 and in the experiment, no gas was utilized. ITS v5r Electrical Impedance Tomography system was applied to acquire the boundary voltages of oil-water two-phase flow. Paraflex HT9 refined oil and aqueous solution of Magnesium Sulphate were used as the dispersed and continuous phase medium, respectively. When the mixed oil and water fluid cyclically flow through the experimental section, the boundary voltages are measured by dual layers ERT sensor and in this way, the oil-water two-phase flow data set is established.

It should be mentioned that the device can only measure the volume fraction with a certain range for oil-water two-phase flow [12], because when the volume fraction is more than 0.5, the mixed liquid which oil becomes the continuous phase will affect the current excitation of the sensor, resulting in the measured voltages to be inaccurate.

Detailed experimental procedures are described in [12].

B. *Data Preprocessing*

The measurement voltages are obtained from 33 cases with a different mixture of oil flow and water flow, and each case includes 2000 sets of data, a total of 66000 EIT measurement voltages and corresponding volume fractions, ranging from 0-0.45, in the oil-water two-phase flow dataset. The VF is calculated by EIT based on (1) and (2). In the paper, the calculated VF from EIT is used as the label. It is also possible to adopt the reference VF provided by NEL or other reliable sensors, such as ultrasonic devices or high-speed cameras.

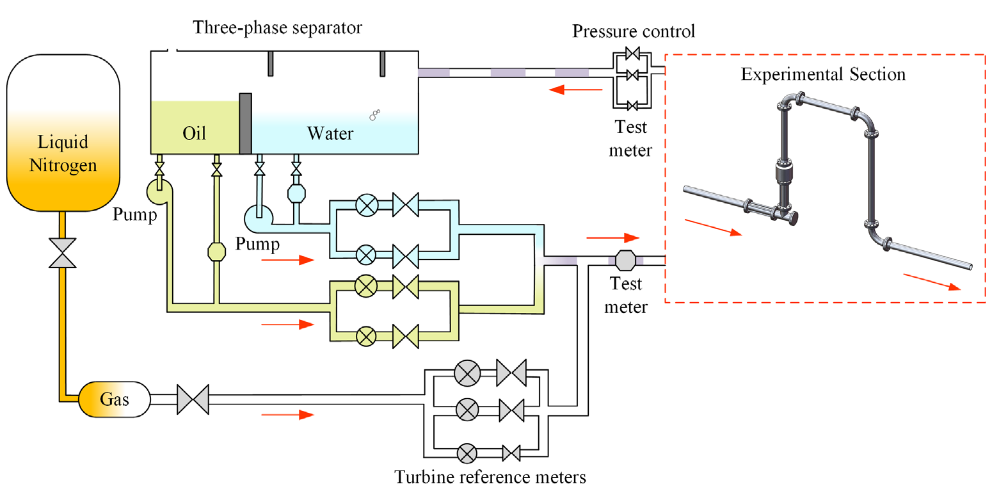

Fig.6. Schematic of TUV NEL multiphase flow facility.

TABLE II

TRAINING TIME AND AVERAGE PREDICTION TIME UNDER DIFFERENT METHODS

Methods	Training time (min)	Average predication time (ms)
SVR	0.01	0.01
LeNet	11.36	1.27
MLCNN	11.40	2.10
ResNet	14.10	3.94
FC	11.34	1.06
UNet-FC	34.23	4.25
AU-FC	26.81	5.33

The dataset is randomly divided into three parts with the proportion of 70% training set, 20% validation set and 10% test. Before fed into the networks, the data is normalized. After normalization, the generality of the network would be greatly improved. The expression is given by,

$$U_i' = \frac{U_i - U_{mean\_tra}}{U_{std\_tra}} \tag{12}$$

where U_i and U_i' are the original and normalized measurement voltages. U_{mean_tra} and U_{std_tra} are the mean value and standard deviation of the training set.

It should be mentioned that the measurement voltages in validation and test sets are also normalized by U_{mean_tra} and U_{std_tra}. In the oil-water two-phase flow dataset, the volume fraction measured by EIT is ranged from 0-0.45, so it is not necessary to normalize them anymore.

C. Evaluation Metrics

Three regression metrics: Mean Squared Error (MSE), Mean Absolute Error (MAE) and Mean Absolute Percentage Error (MAPE) are adopted to quantitatively analyze the volume fraction prediction ability under different methods. MAE, similar to MSE, evaluates the absolute value of the deviation between the real value and the predicted one; while MAPE evaluates the relative value of the deviation. The closer the indicators are to 0, the more accurate the prediction is. The definition of these regression metrics are as follows,

$$MSE = \frac{1}{n}\sum_{i=1}^{n}(\hat{\alpha}_i - \alpha_i)^2 \tag{13}$$

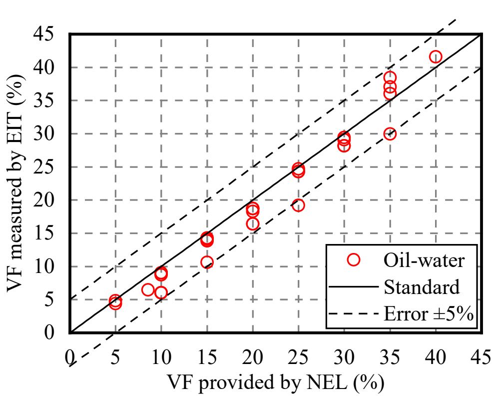

Fig.7. Comparison between VF measured by EIT and VF provided by NEL.

TABLE III

EVALUATION METRICS UNDER DIFFERENT METHODS

Methods	MSE	MAE	MAPE (%)
SVR	16.30	3.43	33.93
LeNet	3.43	1.11	6.11
MLCNN	1.00	0.27	1.27
ResNet	0.61	0.10	0.48
FC	26.23	3.30	18.58
UNet-FC	1.24	0.17	0.80
AU-FC	**0.59**	**0.08**	**0.35**

*Best results are highlighted in bold.

$$MAE = \frac{1}{n}\sum_{i=1}^{n}\left|\hat{\alpha}_i - \alpha_i\right| \tag{14}$$

$$MAPE = \frac{100\%}{n}\sum_{i=1}^{n}\left|\frac{\hat{\alpha}_i - \alpha_i}{\alpha_i}\right| \tag{15}$$

where n is the total number in the validation set or test set.

D. Training Setting

Support Vector Regression (SVR) is based on Sklearn, and the deep learning methods are implemented in the Pytorch environment. All the methods were run in the computer with NVidia GeForce RTX 2070 8GB GPU, Intel Core i7-9700K CPU (3.6 GHz) and 32 GB RAM. For the SVR method, the optimized parameters-penalty coefficient is adjusted to 2 and 0.002 for the kernel coefficient. For the AU-FC deep learning method, Adam [38] is adopted as the optimizer and warm-up strategy [39] is selected to balance the convergence of initial network training and the speed of network training. The warm-up stage lasts for 10 epochs with a linear increase of learning rate from 5×10^{-5} to 5×10^{-4}, and then the learning rate decays by 0.1 every 20 epochs. The maximum number of epochs is 100 in the training process. The batch size is set to 200, and the weight decay, l_2 regularization term, is set to 10^{-5} to avoid overfitting. Random initialization is adopted. The hyperparameters of other deep learning methods mentioned above are carefully optimized by empirical and manual parameters search. Finally, the epoch with the smallest loss in the validation set is selected as the optimal epoch for the test set.

IV. RESULTS AND DISCUSSION

For 33 cases, the comparison between VF measured by EIT and that provided by NEL is shown in Fig. 7. Similarly to the conclusion drawn from [12], the VF provided by NEL is slightly larger than that measured by EIT when the VF is between 0 to 0.3, and when the VF is out of range 0-0.3, the value is overestimated compared with that of NEL. The reason that we didn't select the VF from the readings of the valves on TUV NEL facility as reference in the training process is that those VFs are calculated based on the superficial flow rates of oil and water before mixing, not the true local VF at the testing section. Because of the slip between oil and water, the VF based on the superficial flow rates of oil and water tends to be overestimated. When the VF is larger than 0.35, the oil-water flow ends water continuous phase, where EIT cannot provide

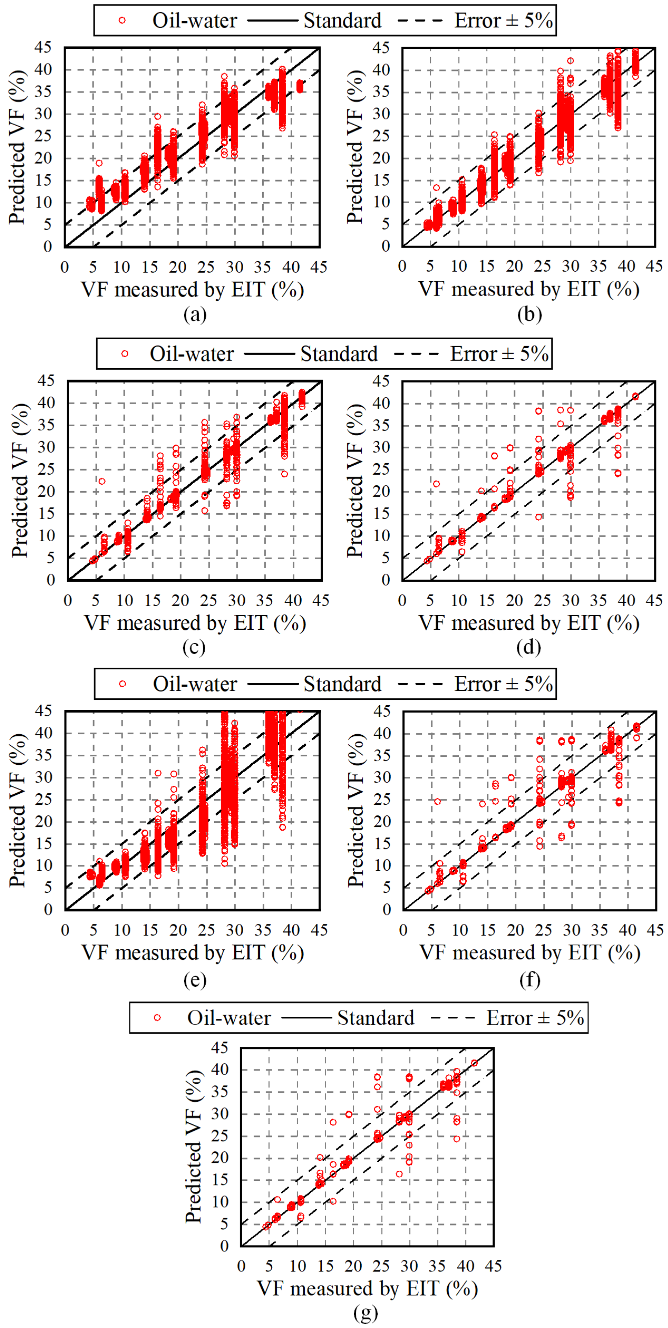

Fig.8. Predicted oil volume fraction under different methods. (a) SVR. (b) LeNet. (c) MLCNN. (d) ResNet. (e) FC. (f) UNet-FC. (g) AU-FC.

reliable results anymore. However, although there are some differences in VF in quantitative analysis, it can still be seen from Fig. 7 in qualitative analysis that the volume fraction by two methods has the same change trend. Besides, the error is almost within ±5%. Possible reason for abnormal values is measurement errors in the instrument.

The training time and average prediction time per set of data for different methods are shown in Table II. The UNet-FC method consumes the most training time (34.23 minutes). Due to the shallower structure of LeNet, MLCNN, ResNet and FC networks, the training time of these methods is faster than UNet-FC and AU-FC, which have similar training time. Since the parameter setting is optimized by empirical method without

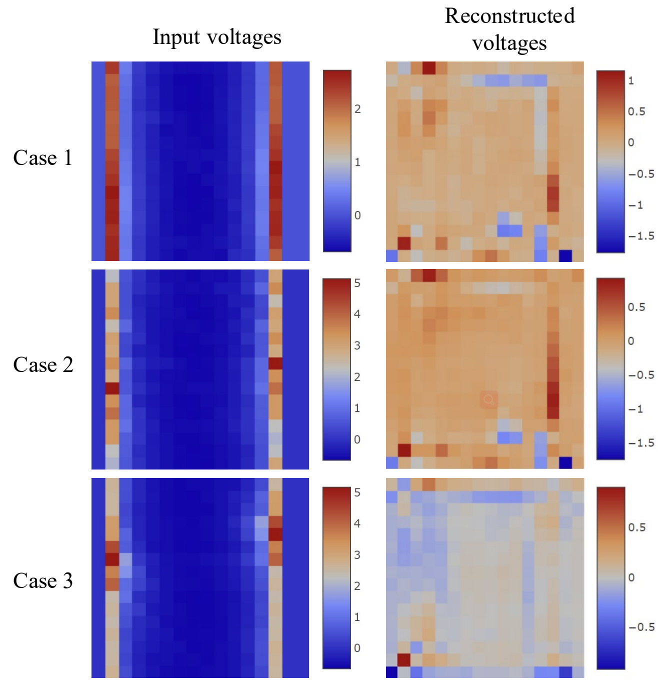

Fig.9. The reconstructed multiscale voltages by AU-FC.

iterative process, SVR method has the shortest training time. In terms of average prediction time per set of data, all the methods can be executed within 6 ms, which is fast enough to be applied in the industrial facility for monitoring the volume fraction change in real-time. Among them, the prediction time of SVR is the shortest with 0.01 ms, and that of AU-FC is the longest with 5.33 ms. Considering that the implementation of the methods is an offline training and online prediction process, as long as the training time is within a reasonable range, the prediction performance is the main concern. 34 minutes of training time is acceptable in the work.

Comparisons between the oil volume fraction measured by EIT and the predicted oil volume fraction under different methods are shown in Fig. 8. On qualitative analysis, it can be seen that predicted VF shares the same change trend with VF measured by EIT. The slope between predicted VF and measured VF is nearly 1 for the AU-FC method and the scattered points are mainly concentrated near the standard line. Due to the existence of the attention mechanism, the network will pay more attention to the local measurement voltages rather than all voltages, thereby extracting deeper voltage information, thus making the red cycles are more clustered around the standard line, compared with SVR, LeNet, MLCNN, ResNet, FC and UNet-FC methods. The performance difference between methods is mainly due to the differences in network depth between networks, attention mechanism, residual connection, etc. Furthermore, the VF predicted by AU-FC and that calculated by EIT are consistent in the overall trend within the ±5% error range, but still some differences in scattered data points. These errors mainly come from the measurement error of the equipment and the estimation error of the prediction model.

The quantitative analysis results are shown in Table III. The AU-FC outperforms SVR, LeNet, MLCNN, ResNet, FC and

UNet-FC methods in predicting VF for oil-water two-phase flow with the smallest MSE 0.59, MAE 0.08 and MAPE 0.35%. By suppressing irrelevant areas in the input voltage data and highlighting salient features in specific local areas, the attention module allows the network to focus on important information and learn it fully, thus giving the network a deeper learning depth and improving the predictive performance of the VF. As the baseline, FC method reveals the necessarility of reconstructed multiscale voltages. By multiscale voltages which include deeper features, the prediction results are more accurate. Besides, the prediction results of UNet-FC prove the effectiveness of additive attention gate and compared with UNet-FC method, the MSE of AU-UC decreases from 1.24 to 0.59, the MAE is from 0.17 to 0.08 and MAPE is from 0.80% to 0.35%. Due to the residual connection structure of ResNet, the prediction network retains the original state of the gradient during the backpropagation process, which reduces the risk of gradient disappearance or gradient explosion in the network, thereby making the prediction network more effective and precise. The prediction performance of ResNet, with MSE 0.61, MAE 0.10 and MAPE 0.48%, ranks second among all introduced methods, followed by UNet-FC, MLCNN, LeNet, SVR and FC methods. Besides, due to the shallow structure of LeNet and MLCNN networks, the prediction performances are general.

Reconstructed multiscale voltages by AU-FC of three oil-water two-phase flow cases, with 24.70%, 28.17% and 38.45% VF are shown in Fig. 9. After the voltage reconstruction process, the reconstructed multi-scale voltage variation range of the input voltage will be smaller and some reconstructed voltage areas are highlighted. In three cases, the predicted VF are 24.71%, 28.22% and 38.41%, respectively.

V. Conclusion

In the work, a supervised attention UNet-fully connected network is proposed to directly predict the volume fraction of oil-water two-phase flow with EIT measurement voltages as input. The proposed method copes with the problem of measuring reference voltages, which is costly and time-consuming. Oil-water two-phase flow experiments are carried out to collect EIT boundary voltages based on the TUV NEL facility. Compared with six competitive machine learning methods: SVR, LeNet, MLCNN, ResNet, FC and UNet-FC, the proposed method has a better performance in terms of MSE, MAE and MAPE regression indexes with 0.59, 0.08 and 0.35% respectively. The proposed method increases the feasibility and applicability of EIT combined with the deep learning method in the industrial field. In the future work, we will explore multitask deep learning method to predict the flow category, flow velocity and volume fraction for two-phase flow in one network.

References

[1] N. Jin, C. Yu, Y. Han, Q. Yang, Y. Ren, and L. Zhai, "The Performance Characteristics of Electromagnetic Flowmeter in Vertical Low-Velocity Oil-Water Two-Phase Flow," *IEEE Sens. J.*, vol. 21, no. 1, pp. 464–475, 2021.

[2] X. Dong, C. Tan, Y. Yuan, and F. Dong, "Measuring Oil-Water Two-Phase Flow Velocity with Continuous-Wave Ultrasound Doppler Sensor and Drift-Flux Model," *IEEE Trans. Instrum. Meas.*, vol. 65, no. 5, pp. 1098–1107, 2016.

[3] R. Hilfer, "Modeling and simulation of macrocapillarity," *AIP Conf. Proc.*, vol. 1091, pp. 141–150, 2009.

[4] L. S. Zhai, N. De Jin, Z. K. Gao, Z. Y. Wang, and D. M. Li, "The ultrasonic measurement of high water volume fraction in dispersed oil-in-water flows," *Chem. Eng. Sci.*, vol. 94, pp. 271–283, 2013.

[5] G. Oddie, H. Shi, L. J. Durlofsky, K. Aziz, B. Pfeffer, and J. A. Holmes, "Experimental study of two and three phase flows in large diameter inclined pipes," *Int. J. Multiph. Flow*, vol. 29, no. 4, pp. 527–558, 2003.

[6] G. P. Lucas and N. Panagiotopoulos, "Oil volume fraction and velocity profiles in vertical, bubbly oil-in-water flows," *Flow Meas. Instrum.*, vol. 20, no. 3, pp. 127–135, 2009.

[7] G. H. Roshani, A. Karami, E. Nazemi, and F. Shama, "Volume fraction determination of the annular three-phase flow of gas-oil-water using adaptive neuro-fuzzy inference system," *Comput. Appl. Math.*, vol. 37, no. 4, pp. 4321–4341, 2018.

[8] H. Yu, C. Tan, H. Wu, and F. Dong, "Oil Fraction Measurement of Nonuniform Dispersed Oil-Water Two-Phase Flow Based on Ultrasonic Attenuation," *IEEE Trans. Instrum. Meas.*, vol. 70, pp. 1–13, 2021.

[9] J. Zhang, J. yu Xu, Y. xiang Wu, D. hui Li, and H. Li, "Experimental validation of the calculation of phase holdup for an oil-water two-phase vertical flow based on the measurement of pressure drops," *Flow Meas. Instrum.*, vol. 31, pp. 96–101, 2013.

[10] C. Tan, W. Dai, H. Wu, and F. Dong, "A conductance ring coupled cone meter for oil-water two-phase flow measurement," *IEEE Sens. J.*, vol. 14, no. 4, pp. 1244–1252, 2014.

[11] M. Sharifzadeh, H. Khalafi, H. Afarideh, and R. Gholipour, "Determination of oil–water volume fraction by using a pencil-beam collimated gamma-ray emitting source in a homogenized flow regime condition," *Flow Meas. Instrum.*, vol. 52, no. October 2015, pp. 17–24, 2016.

[12] J. Jia, H. Wang, and D. Millington, "Electrical Resistance Tomography Sensor for Highly Conductive Oil-Water Two-Phase Flow Measurement," *IEEE Sens. J.*, vol. 17, no. 24, pp. 8224–8233, 2017.

[13] C. Olerni, J. Jia, and M. Wang, "Measurement of air distribution and void fraction of an upwards air-water flow using electrical resistance tomography and a wire-mesh sensor," *Meas. Sci. Technol.*, vol. 24, no. 3, p. 035403, 2013.

[14] Z. Cui, Q. Zhang, K. Gao, Z. Xia, and H. Wang, "Electrical Impedance Sensors for Multi-phase Flow Measurement: A Review," *IEEE Sens. J.*, vol. 21, no. 24, pp. 1–16, 2021.

[15] M. Lukaschewitsch, P. Maass, and M. Pidcock, "Tikhonov regularization for electrical impedance tomography on unbounded domains," *Inverse Probl.*, vol. 19, no. 3, pp. 585–610, 2003.

[16] H. Zhu, J. Sun, L. Xu, W. Tian, and S. Sun, "Permittivity Reconstruction in Electrical Capacitance Tomography Based on Visual Representation of Deep Neural Network," *IEEE Sens. J.*, vol. 20, no. 9, pp. 4803–4815, 2020.

[17] L. Yang, H. Wu, K. Liu, B. Chen, W. Han, and J. Yao, "Image Reconstruction Improvement with Optimal Driven-Measurement Pattern Selection for Electrical Impedance Tomography," *IEEE Sens. J.*, vol. 21, no. 12, pp. 13530–13539, 2021.

[18] J. Jia, M. Wang, and Y. Faraj, "Evaluation of EIT systems and algorithms for handling full void fraction range in two-phase flow measurement," *Meas. Sci. Technol.*, vol. 26, no. 1, p. 15305, 2015.

[19] C. Olerni, J. Jia, and M. Wang, "Measurement of air distribution and void fraction of an upwards air-water flow using electrical resistance tomography and a wire-mesh sensor," *Meas. Sci. Technol.*, vol. 24, no. 3, 2013.

[20] Z. Xu, Y. Jiang, B. Wang, H. Ji, and Z. Huang, "Void fraction measurement of gas – liquid two-phase flow with a 12-electrode contactless resistivity array sensor," *Meas. Sci. Technol.*, vol. 31, no. 11, p. 115103, 2020.

[21] Z. Wang, S. Yue, X. Liu, A. McEwan, B. Sun, and H. Wang, "Estimating Homogeneous Reference Frame for Absolute Electrical Impedance Tomography through Measurements and Scale Feature," *IEEE Trans. Instrum. Meas.*, vol. 70, pp. 1–12, 2021.

[22] Z. Gao *et al.*, "Multitask-Based Temporal-Channelwise CNN for Parameter Prediction of Two-Phase Flows," *IEEE Trans. Ind. Informatics*, vol. 17, no. 9, pp. 6329–6336, 2021.

[23] C. Tan, F. Li, S. Lv, Y. Yang, and F. Dong, "Gas-Liquid Two-Phase Stratified Flow Interface Reconstruction with Sparse Batch Normalization Convolutional Neural Network," *IEEE Sens. J.*, vol. 21, no. 15, pp. 17076–17084, 2021.

[24] S. Azizi, H. Karimi, and P. Darvishi, "Flow pattern and oil holdup prediction in vertical oil-water two-phase flow using pressure fluctuation signal," *Iran. J. Chem. Chem. Eng.*, vol. 36, no. 2, pp. 125–141, 2017.
[25] W. Dang, Z. Gao, L. Hou, D. Lv, S. Qiu, and G. Chen, "A Novel Deep Learning Framework for Industrial Multiphase Flow Characterization," *IEEE Trans. Ind. Informatics*, vol. 15, no. 11, pp. 5954–5962, 2019.
[26] X. Chen, H. Hu, J. Zhang, and Q. Zhou, "An ECT system based on improved RBF network and adaptive wavelet image enhancement for solid/gas two-phase flow," *Chinese J. Chem. Eng.*, vol. 20, no. 2, pp. 359–367, 2012.
[27] L. Zhu, Y. Jiang, Y. Li, W. Lu, and M. Zhang, "Conductivity Prediction and Image Reconstruction of Complex-Valued Multi-Frequency Electrical Capacitance Tomography Based on Deep Neural Network," *IEEE Trans. Instrum. Meas.*, vol. 71, no. 1, pp. 1–10, 2022.
[28] Z. Xu, F. Wu, X. Yang, and Y. Li, "Measurement of gas-oil two-phase flow patterns by using CNN algorithm based on dual ECT sensors with venturi tube," *Sensors (Switzerland)*, vol. 20, no. 4, p. 1200, 2020.
[29] O. Oktay *et al.*, "Attention U-Net: Learning Where to Look for the Pancreas," no. Midl, 2018.
[30] Z. Liu, P. Bagnaninchi, and Y. Yang, "Impedance-optical Dual-modal Cell Culture Imaging with Learning-based Information Fusion," *IEEE Trans. Med. Imaging*, p. doi: 10.1109/TMI.2021.3129739., 2021.
[31] M. Wang, "Inverse solutions for electrical impedance tomography based on conjugate gradients methods," *Meas. Sci. Technol.*, vol. 13, no. 1, pp. 101–117, 2002.
[32] C. Tan, S. Lv, F. Dong, and M. Takei, "Image Reconstruction Based on Convolutional Neural Network for Electrical Resistance Tomography," *IEEE Sens. J.*, vol. 19, no. 1, pp. 196–204, 2019.
[33] A. Malik, Y. Tikhamarine, D. Souag-Gamane, O. Kisi, and Q. B. Pham, "Support vector regression optimized by meta-heuristic algorithms for daily streamflow prediction," *Stoch. Environ. Res. Risk Assess.*, vol. 34, no. 11, pp. 1755–1773, 2020.
[34] Y. Lecun, L. Bottou, Y. Bengio, and P. Haffner, "Gradient-based learning applied to document recognition," *Proc. IEEE*, vol. 86, no. 11, pp. 2278–2324, 1998.
[35] K. Simonyan and A. Zisserman, "Very deep convolutional networks for large-scale image recognition," *3rd Int. Conf. Learn. Represent. ICLR 2015 - Conf. Track Proc.*, pp. 1–14, 2015.
[36] K. He, X. Zhang, S. Ren, and J. Sun, "Deep residual learning for image recognition," *Proc. IEEE Comput. Soc. Conf. Comput. Vis. Pattern Recognit.*, pp. 770–778, 2016.
[37] Z. Chen, Y. Yang, J. Jia, and P. Bagnaninchi, "Deep learning based cell imaging with electrical impedance tomography," *I2MTC 2020 - Int. Instrum. Meas. Technol. Conf. Proc.*, no. May, pp. 1–6, 2020.
[38] S. Bock and M. Weis, "A Proof of Local Convergence for the Adam Optimizer," *Proc. Int. Jt. Conf. Neural Networks*, no. July, pp. 1–8, 2019.
[39] P. Goyal *et al.*, "Accurate, Large Minibatch SGD: Training ImageNet in 1 Hour," 2017.

Hao Yu was born in Heilongjiang Province, China, in 1996. He received the B.S. degrees in electrical engineering from North China Electric Power University, Bao Ding, China, in 2018, and the M.Sc. degree in electrical engineering from Harbin Institute of Technology, Harbin, China, in 2020. He is currently pursuing the Ph.D. degree with the Agile Tomography, School of Engineering, The University of Edinburgh.
His research interests include disturbance rejection control, deep learning for electrical impedance tomography in industrial and medical field.

Zhixi Zhang was born in Jilin Province, China, in 1996. She obtained the B.Eng. degree from the School of Engineering and North China Electric Power University in July 2018. She started as a Ph.D. student in the Agile Tomography group, School of Engineering, The University of Edinburgh, in September 2018.
Her research interests include motion control, electrical impedance tomography.

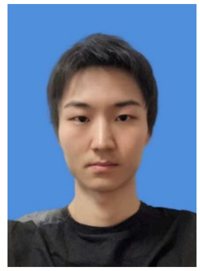

Yang Gao was born in Anhui Province, China, in 1996. He received B.S. Degree in Internet of Things from National University of Ireland Dublin college in 2018, and the M.Sc Degree in Electrical and Electronic Engineering from Durham University in 2020. He is pursuing his Ph.D. with the deep learning, School of Engineering, The University of Edinburgh.
He focuses on computer vision and deep learning algorithm research.

Jiabin Jia (Senior Member, IEEE) received the B.Eng. and M.S. degrees in electrical and electronics engineering from Wuhan University, Wuhan, China, in 2002 and 2005, respectively, and the Ph.D. degree from the University of Leeds, Leeds, U.K., supported by the Overseas Research Students Award Scheme in 2010.
He served as a Hardware Engineer at H3C Technology Company, Ltd., Hangzhou, China, in 2006. Following three years working on an EPSRC project as a Research Fellow, he was appointed as a Lecturer at the School of Engineering, The University of Edinburgh, Edinburgh, U.K., in 2013. His current research interests include electrical tomography, acoustic tomography, multiphase flow measurement, and medical imaging. He has authored more than 30 peer-reviewed journal papers and has contributed to and led a range of research projects.